Multiple Contrail Streamers Observed by Radar

THOMAS G. KONRAD AND JOHN C. HOWARD

Applied Physics Laboratory, The Johns Hopkins University, Silver Spring, Md. 20910

(Manuscript received 6 November 1973)

ABSTRACT

An unusual case of multiple streamers or filaments with the characteristic mare's tail pattern in vertical section has been observed by radar where the generating elements were condensation trails laid by high-altitude aircraft. The contrails were laid perpendicular to the wind and as they drifted a multitude of streamers formed along each trail. The streamers extended from 9 km to the ground. Numerous contrails were observed, each of which produced a sheet of streamers. RHI and PPI photographs at X and S band taken over a 2-hr period show the three-dimensional shape of the streamers due to the wind shear. Doppler measurements were also taken. The resulting velocity spectra are very narrow indicating little or no turbulence. Reflectivity factors were measured at various altitudes and show a decrease in reflectivity with distance from the generating line. Fall velocities based on the slopes of the streamer patterns varied from 0.4 to 1.4 m sec^{-1}. In general, the characteristics of the precipitation streamers were quite similar to those previously measured in naturally occurring cloud forms such as cirrus uncinus.

1. Introduction

The patterns and characteristics of precipitation from generating cells above the melting layer and the resulting precipitation trails or streamers have been observed and interpreted by a number of investigators for some time (e.g., Browne, 1952; Marshall, 1953; Miles, 1956; Langleben, 1956; Atlas, 1957; among others).

The precipitation streamers form part of the familiar mare's tail pattern of cirrus uncinus clouds. The trails are produced by compact generating elements which move with the wind at their altitude. In the case of a unidirectional wind field with constant shear, the form of the trails is parabolic. The whole trail pattern moves with the horizontal velocity of the generating element. The results and interpretations by various investigators are summarized in Marshall *et al.* (1955) and Mason (1971), and will not be reviewed here.

All the studies reported to date, however, were concerned with the characteristics of generating cells occurring naturally in the atmosphere. This paper discusses a set of observations where the generating elements were condensation trails laid by high-altitude jet aircraft. To the authors' knowledge, this is the first time that streamers produced by condensation trails have been observed by radar. As the contrails drifted with the wind, a multitude of filaments or streamers were formed from each contrail. These were observed both visually and by radar.

2. The observations

The observations of the contrail streamers were made on 12 February 1971 at Wallops Island, Va., using the high-power, narrow-beam X and S band radars of the NASA Radar Atmospheric Research Facility. The detailed characteristics of these radars are contained in NCAR (1969). Briefly, the S band (10.7 cm) radar is a monopulse tracking radar with a beamwidth of 0.4° and a peak power of 3 MW. On this day, a 1.3-μsec pulse with a pulse repetition frequency (prf) of 960 sec^{-1} were used. The X band (3.2 cm) radar has an 0.2° beam, and transmits 1 MW peak power. The prf and pulse length are fixed at 320 sec^{-1} and 2 μsec, respectively. Simultaneous range height and plan position indicator (RHI and PPI) photographs may be made since the X band mount is slaved to the S band.

Radar observations began at 0840 with the first contrail streamers detected around 1000 (all times Eastern Standard). The radar patterns were recorded on RHI and PPI pictures continuously for the next 2 hr. Stepped-azimuth RHI series along with stepped-elevation PPI's were taken.

Quantitative radar data were also taken in the form of Doppler from ten data gates at S band. On four occasions, the Doppler returns from the streamers at various altitudes and ranges were recorded on magnetic tape. The data were taken in the searchlight mode, i.e., with fixed antenna and data-gate positions. Data gates, 0.4 μsec long, were spaced 1.4 μsec apart, leading edge to leading edge.

The radars are located ~2 mi from the shoreline. A commercial jet route running roughly NNE–SSW is just to the west of the radar facility. To the east is a NASA controlled area which no aircraft may enter without prior approval. During the morning hours, high-altitude commercial jet aircraft laid condensation

FIG. 1. Photograph taken at 1155 EST to the southwest showing streamers from an old contrail and a new contrail being laid along the commercial airway.

FIG. 3. Photograph to the east over the NASA controlled area showing contrails which have drifted eastward while retaining their NE–SW orientation.

trails along the route at altitudes from 9–10 km. Sky photographs were taken throughout the morning and, in many instances, show the trail being laid with the aircraft in the picture (see Figs. 1 and 2).

The wind was generally from the west so that the trails drifted eastward but retained their NNE–SSW orientation. This is illustrated in Fig. 3 which was taken to the east over the NASA restricted area around 1200.

As the trails drifted eastward, they acted as generating lines. Each trail produced multiple streamers or filaments which were oriented generally along an E–W direction, i.e., along the wind. Figs. 4 and 5 were taken almost overhead to the west around 1200 and show the contrails with the individual streamers emanating from what appear to be clumps in the contrail itself. These photographs are quite similar to those taken from an aircraft during a study of the

FIG. 4. Photograph of individual streamers taken overhead at 1155. Aircraft is at low altitude and is not laying a contrail.

FIG. 2. As in Fig. 1 except for photograph at 1122 EST.

FIG. 5. Photograph to the west showing streamers aligned perpendicular to the contrails.

FIG. 6. Photograph to the southwest at 1321 EST showing thin cirrus cloud cover. By this time the sky is practically overcast. Note contrail being laid in upper left.

properties of cirrus generating cells (Heymsfield and Knollenberg, 1972; Knollenberg, 1972). The striking resemblance between the contrail streamers and cirrus uncinus clouds is evident in the photographs shown both here and in Knollenberg (1972).

In the early morning hours (e.g., 0800–0900) the sky was clear with no lower or middle clouds and only a trace of thin cirrus around 9 km. An RB-57 aircraft was working with the radar in a study of turbulent layers. The aircraft confirmed the lack of clouds except for the thin cirrus. In addition, no turbulence was reported during repeated soundings except for a very light patch at 6.6 km.

As the morning progressed and contrails continued to be laid, the sky became filled with cirrus resulting from the contrails and filaments. Fig. 6 is a photograph taken to the SSW at 1220 showing the sky virtually covered with the thin cirrus. Note that the streaked appearance of the cirrus is in an E–W direction while the contrails in the upper left and lower right hand corners of the photograph are approximately N–S. This continual buildup of the cirrus was also reported by the RB-57 aircraft.

In midmorning a radiosonde sounding was made and is shown in Fig. 7. The air was stable at all altitudes with low humidity. This is consistent with the results of Gunn *et al.* (1954) and Douglas *et al.* (1957) where it was found that precipitation streaks were most frequent and well defined when the air aloft was stable.

Appleman (1953) developed criteria for contrail formation as a function of the type of fuel and the atmospheric condition. Fig. 8 shows a graph of the required relative humidity for contrail formation as a function of altitude along with the radiosonde sounding data. Contrails will form only if the ambient relative humidity is equal to, or greater than, the value indicated at that point in the sounding. In the present set of observations, the contrails in fact formed at temperatures several degrees warmer than that predicted by Appleman for the measured relative humidity. (Conversely, they formed at relative humidities much less than that required for the measured temperature.) Knollenberg (1972) found a similar result. He notes that not all the energy from fuel combustion appears as heat immediately as assumed by Appleman and others. He also points to the perturbations in temperature and pressure brought about

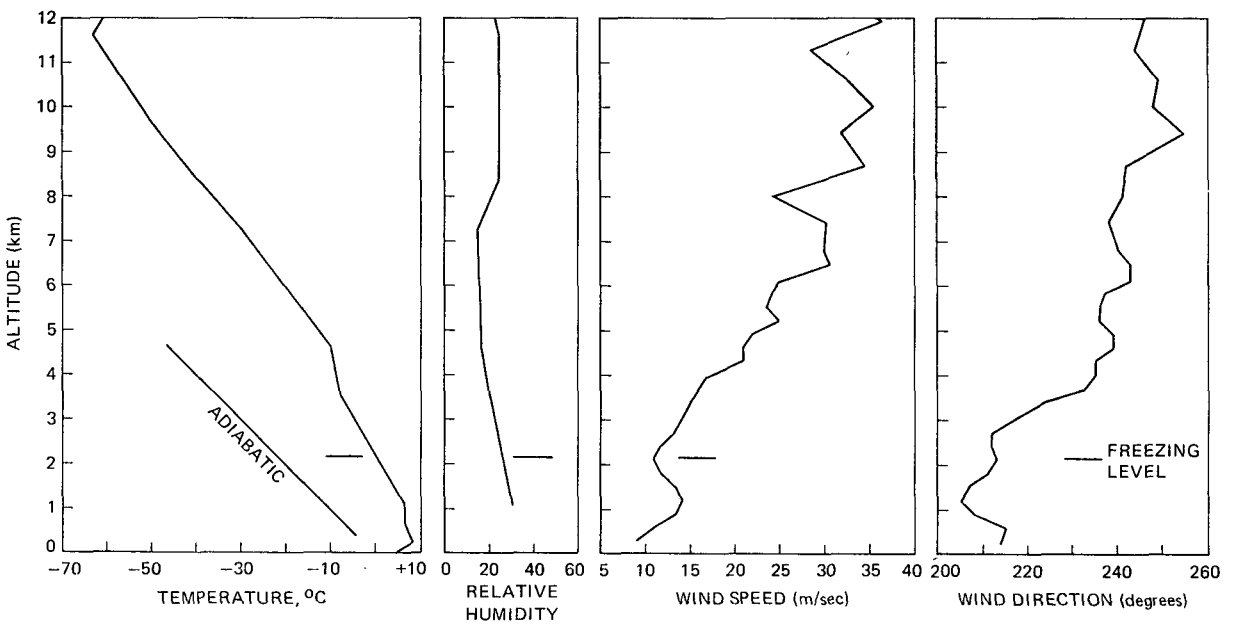

FIG. 7. Radiosonde sounding taken at 1010 EST from Wallops Island.

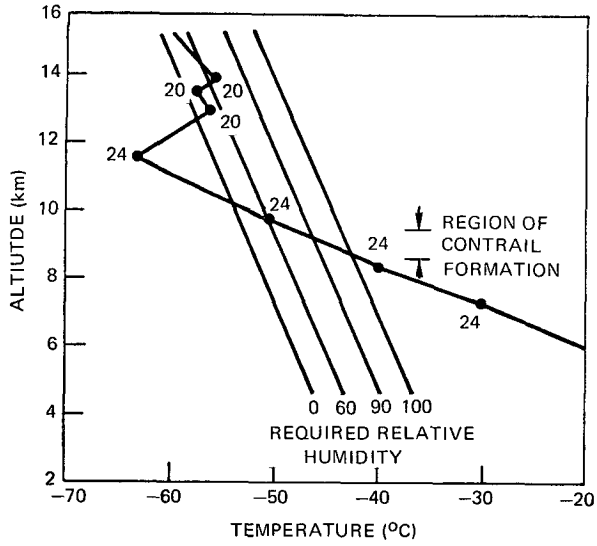

FIG. 8. Comparison of atmospheric conditions with required conditions for contrail formation from Appleman (1953). Numbers beside points are relative humidity from radiosonde sounding. Note that the contrails formed at temperatures several degrees warmer than predicted. See text.

by the trailing vortex pair and the unequal mixing of heat and water vapor as being sufficient, perhaps, to cause deviations from the theoretically derived prediction curves. In any case, the contrails were formed and persisted for long periods as will be discussed below.

3. Results and discussion

a. Radar patterns

The radar patterns in the vertical are similar to those found by earlier investigators such as Marshall (1953), Miles (1956), and Douglas *et al.* (1957) in naturally occurring cirrus, although considerably more complicated due to the three-dimensionality of the wind field and the multiplicity of the streamers. It should be noted that the majority of earlier observations were made using time-height presentations with the radar beam pointed vertically, while the present observations were made using RHI type vertical sections. The interpretation and analysis of the two techniques is slightly different. Fig. 9 is a set of RHI sections taken at different azimuth angles through the same sheet of filaments within 8 min of each other. Two distinct characteristics are evident. First, there is the "S" shape to the patterns around 6–8 km. This corresponds to the nose in the wind speed at these altitudes shown in Fig. 7. Second is the strong sensitivity of the patterns to azimuth angle. This is simply due to the three-dimensionality of the trail caused by the wind field and the multiplicity of streamers being cut by the RHI vertical plane. If the wind field were unidirectional, then the complete pattern from a generating cell to the ground would be contained in a single vertical plane. In the present case, however, the wind direction varied continuously with altitude and the pattern of each filament trail is three dimensional. Thus, a single RHI will cut various filaments at various altitudes and at various angles. No single vertical plane will contain the whole trail; rather, it will intersect the trail at a point. The effects of a three-dimensional wind field on the radar patterns is discussed by a number of authors including Marshall (1953), Miles (1956), and Douglas *et al.* (1957). They are most graphically illustrated in the PPI photographs such as Fig. 10, an expanded PPI sector scan to the east of the radar, and subsequent figures of PPI photographs.

The long-filament patterns were always found to the east of the radar. The returns to the west were invariably at short range and were not extended. This is due to the fact that in the eastern sector the radar beam is looking up and along the filament while in the west the beam is cutting across the filament; the situation is similar to that of an RHI taken across the sheet of filaments as discussed above.

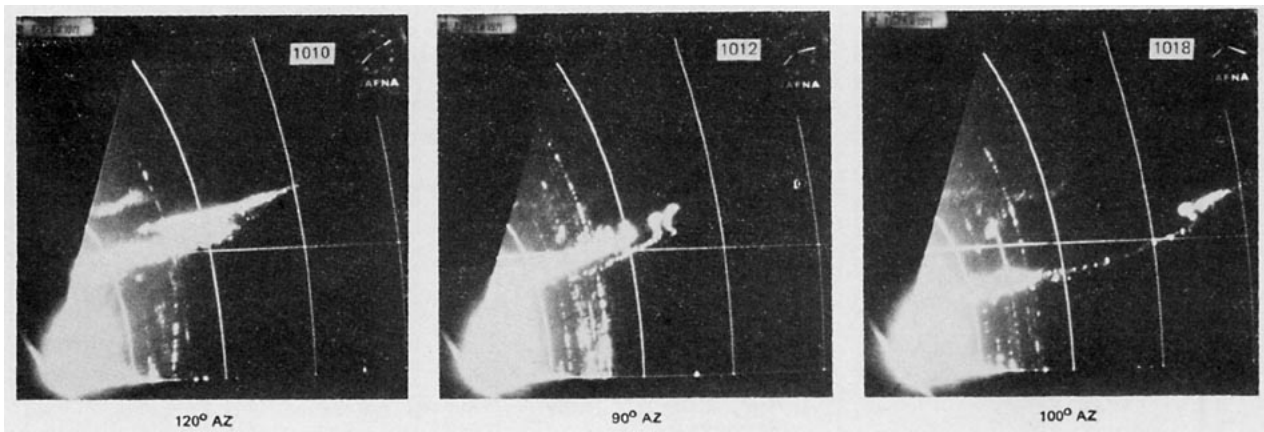

FIG. 9. RHI S band photographs at different azimuth angles through the same streamer sheet. Clock is in GMT with EST shown in box. Note pronounced S shape to pattern. Height marker is at 20,000 ft (6.1 km), range marks at every 5 n mi (18.5 km).

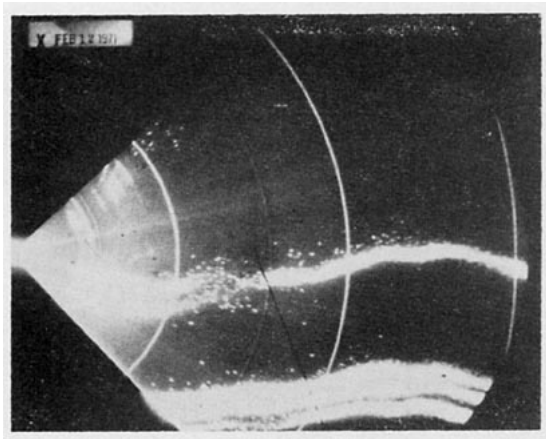

FIG. 10. Expanded X band PPI sector photograph showing effect of wind directional shear on the streamer. Elevation angle was 6.3° covering 45° to 135° in azimuth. Range marks are every 5 n mi (18.5 km).

The radar patterns on PPI are typically patchy. This is again due to the fact that the radar beam, as it sweeps out a conical slice through the atmosphere, passes through several sheets of filaments at different locations. Fig. 11 shows simultaneous X and S band PPI photographs taken from a stepped-elevation PPI series. A three-dimensional reconstruction shows the multiple sheets of filaments. As an example, the returns labelled A in each photograph are from a single sheet cut at different elevation angles while those labelled B are from another sheet. In this particular series of PPI pictures, at least four separate sheets are positively identifiable, each being the product of a single contrail. Langleben (1956) found similar results using a CAPPI-type display. He interprets the sheets as being from line arrays of generating cells as opposed to a line element as suggested by Lhermitte (1952). Whether a contrail is considered a line array of cells (due to the clumping of the contrail as it ages) or a line element is somewhat moot.

The spacing between the individual filaments is roughly 2 km. This spacing is about half that reported by Langleben (1956) for snow-generating cells occurring naturally in line arrays. His generating elements were found to be approximately 1.6 km in diameter with spacings between filaments from 3.2 to 6.4 km. The mechanism producing the trails in the two cases may well be quite different. In any event, the 2-km spacing between filaments was constant from one sheet to another.

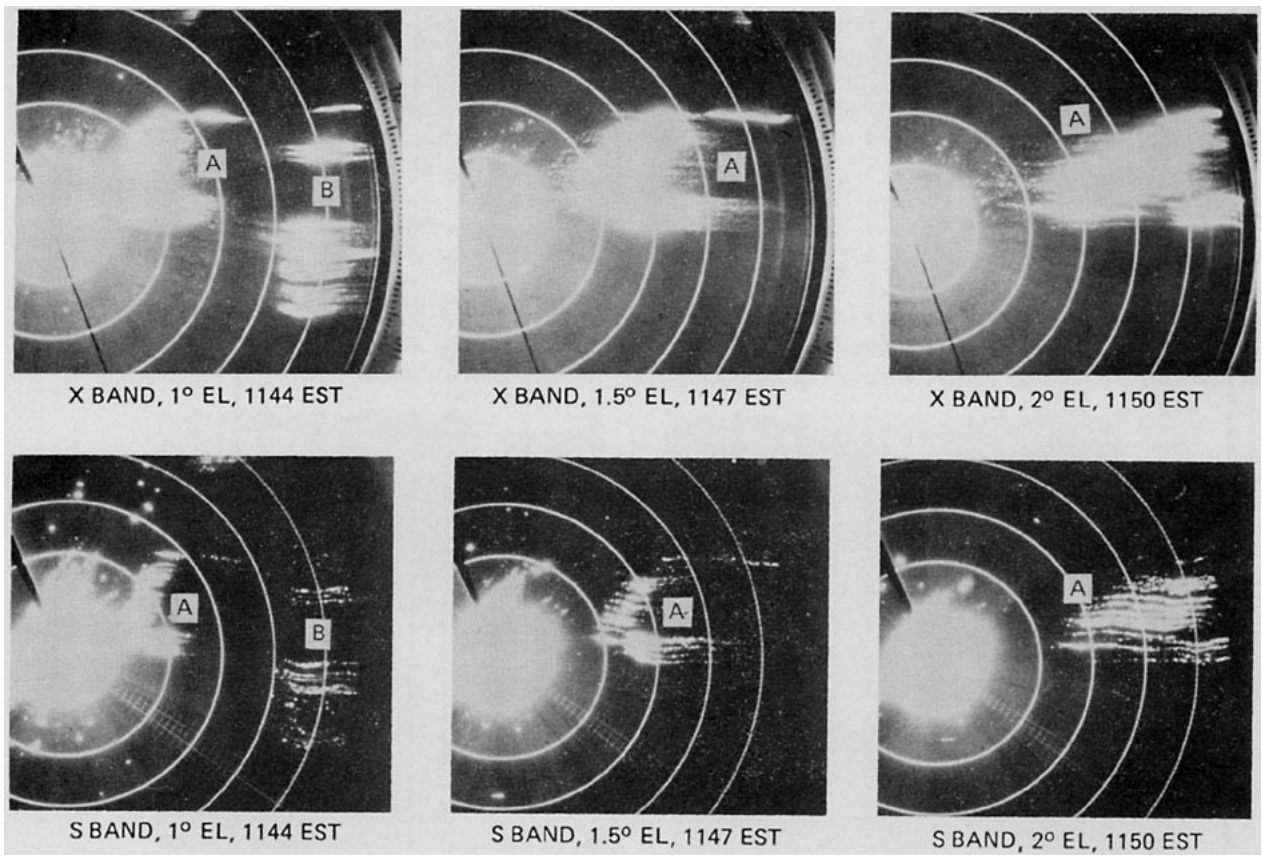

FIG. 11. Simultaneous X and S band PPI photographs at different elevation angles showing streamers from two separate sheets Note dot-like character of S band returns as compared to the strong diffuse returns at X band. Range marks are every 5 n mi (18.5 km).

The radar patterns on the X band photographs (as in Fig. 11) always appear brighter and more diffuse than at S band. One reason, of course, may be scope settings. However, considering the operating conditions for the two radars and assuming beam filling, the power received at X band should be roughly 20 dB higher than at S band for Rayleigh scattering. Further, the X band radar may be seeing many more of the smaller particles than the S band which would also account for the difference in the appearance of the scope displays.

It has not been possible to reconstruct the pattern of a single filament covering the entire altitude range. This is primarily due to the multiplicity of filaments and the difficulty in identifying the same filament from picture to picture with any certainty. In addition, the azimuth increment between RHI's in a raster scan was rather large—10° in some cases. A number of RHI photographs, however, do show returns over the entire altitude range; for example, see Fig. 12. The patterns on X band appear solid, apparently due to the blooming on the scopes. The S band picture, however, shows the patterns to be made up of a number of clumps. Again this is due to the plane of the RHI crossing the sheet of filaments at an angle. In any event, photographs such as these show that the sheet of filaments does extend from the generating level to the ground. This implies that the ice crystals survived a fall of at least 7 km (from the generating level at 9 km to the melting level around 2 km). Using a nominal fallspeed of 1 m sec^{-1} for the particles, such a fall takes roughly 2 hr. In fact, ice crystals from natural cirrus have been observed to survive a fall of this magnitude. Braham and Spyers-Duran (1967) collected crystals in apparently clear air up to 6 km below cirrus using an aircraft. An attempt was made by Braham to explain how the crystals could survive in such an environment and in such concentrations as were measured but the assumptions necessary in the calculations precluded any definitive conclusion or explanation.

Although the returns from the contrail streamers were observed for several hours, no attempt was made to follow a single sheet of filaments from a given contrail for any length of time to determine the lifetime of the generating line, i.e., the contrail. Changes in the mode of radar operation, from RHI to PPI to searchlight, precluded the identification of an individual sheet over an extended period. However, the contrail must have acted as a generating line for at least 2 hr since the filaments extended from the generating level to the ground as discussed above. That is, the generating line was still active and producing a fallout of crystals when particles which had been formed more than 2 hr previously were reaching the ground! Langleben (1956) reported observing several snow cells continuously for 1–2 hr. No decaying stage was evident. He concludes that a constant supply of water vapor was being used to grow the snow crystals.

Several of the authors referenced above (e.g., Marshall, 1953; Gunn and Marshall, 1955; Douglas *et al.*, 1957) have discussed the diffusion of the trail at lower altitudes due to wind shear and the sorting of the ice crystals or snowflakes by size according to their fall velocities. The only evidence of this in the RHI and PPI photographs is the fact that the primary radar patterns at lower altitudes from individual streamers are surrounded by dot-like targets (see Figs. 10–12). This is especially evident on those RHI's where the streamer reaches the ground. Dot echoes appear both above and below the main return. Additional comments on this effect are contained in a subsequent section on the reflectivity measurements.

b. Doppler measurements

On four occasions during the observations, Doppler measurements were taken in ten data gates and

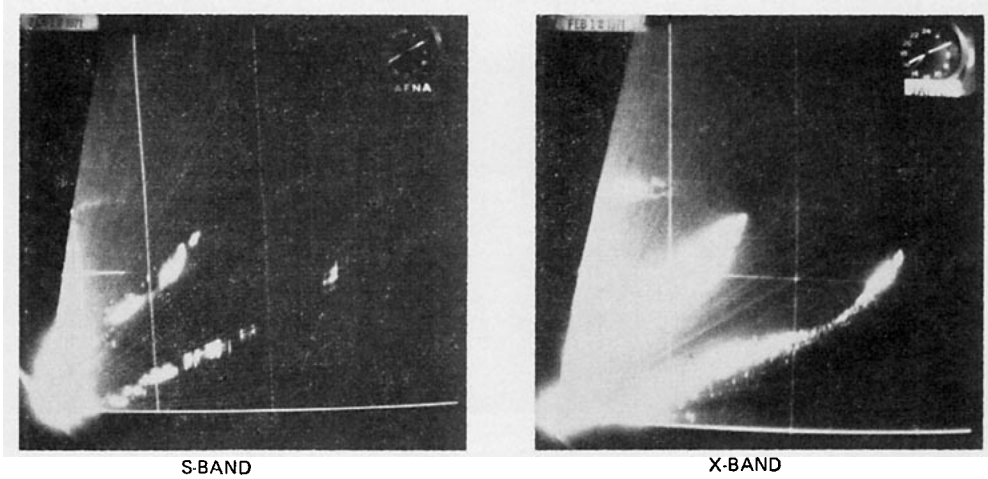

FIG. 12. Simultaneous RHI photographs at X and S band showing streamers extending from the generating level to the ground. Range marks are every 5 n mi (18.5 km) with height marker at 20,000 ft (6.1 km). Photo taken at 1112 EST.

recorded on magnetic tape. The radar beam was fixed in azimuth and elevation. Table 1 shows the conditions and lengths of these runs. The data for each run were divided into consecutive 10-sec intervals and the Doppler spectrum for each interval was calculated. A total of 9600 points were included in each spectrum (radar prf was 960 sec^{-1}). The frequency resolution was 1.25 Hz with 50 degrees of freedom being used in the spectral calculations.

In the vast majority of cases, the individual spectra were very narrow, virtually spikes. The maximum width of the spectra at the noise level was around 10–20 Hz. In a few cases, particularly at low altitudes, the spectra consist of several closely spaced spikes. This lack of spectral width indicates very little atmospheric turbulence. Richardson's numbers calculated using the radiosonde data of Fig. 7 support this conclusion. They were less than 1.0 in only one area, around 6 km, but never dropped below the "critical" value of 0.25 at any altitude. The RB-57 aircraft which had been making soundings just prior to the contrail observations reported very, very light turbulence at 6.6 km during one sounding.

In Fig. 13, the center frequencies of the Doppler spectra for three of the data gates (1, 5 and 10) are compared with the frequency which the radar should have measured based on the radiosonde winds and the azimuth of the radar beam. During each 2-min run, the center frequency varied somewhat from one 10-sec interval to another. The range of this variation is shown in the figure for each gate. The radar samples a volume of space, and the altitude increment covered by the pulse volume is indicated for each gate in Fig. 13.

Now if the pulse volume had been filled with scatterers then the radar Doppler frequencies should have covered a range of values corresponding to that for the altitude increment for a given data gate as shown in Fig. 13. For example, in Run 1, the sampled volume for gate 5 includes an altitude interval from 5.9 to

TABLE 1. Location and time of Doppler measurements with the calculated reflectivity factor.

Run	Gate	Range* (km)	Altitude* (km)	Start time (EST)	Run duration (min)	Reflectivity factor ($mm^6\ m^{-3}$)
1	1			1123:00	2	23
	5	56.3	6.2			45
	10					45
2	1			1131:30	1.5	0.13
	5	31.0	2.2			0.04
	10					0.05
3	1			1133:30	1	0.9
	5	32.9	1.8			0.7
	10					0.8
4	1			1222:10	2	14
	5	125.3	3.1			11
	10					10

* The range and altitude listed are measured to the leading edge of data gate 5.

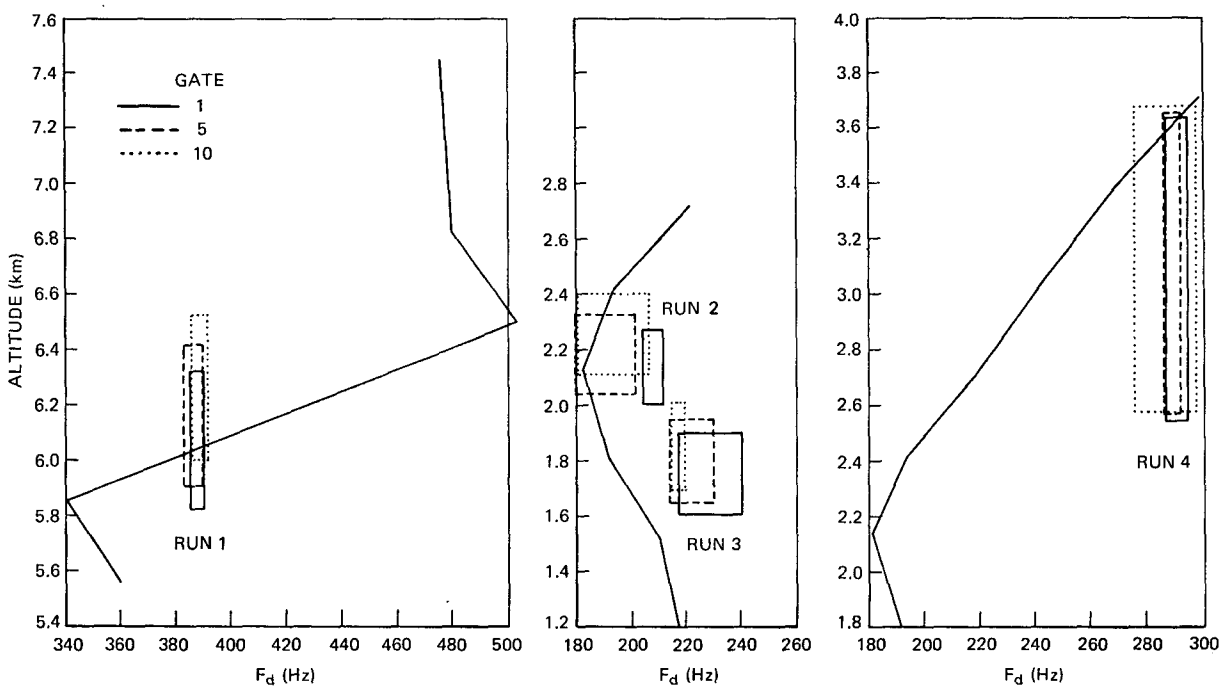

FIG. 13. Comparison of measured frequency of the Doppler spectra with that predicted from the radiosonde data. Boxes indicate range of variation in the center frequency of spectra during a run and the altitude increment included in the pulse volume. Numbers 1, 5 and 10 indicate data gates. See text.

6.4 km. The Doppler frequencies from the radiosonde sounding which should have been measured if the pulse volume were filled are from 350 to 480 Hz, a variation of 130 Hz. However, the radar measured only a narrow range of frequencies around 385 Hz. A similar situation exists in Run 4 where the gated data were taken at long range where the radar beam is very broad. One explanation is that the pulse volumes (the altitude intervals) were not, in fact, filled with scatterers but only some rather small portion; in the case of Run 4 this would be the region around 3.6 km. This lack of beam-filling affects any calculation of reflectivity factor and will be discussed further below. Another explanation is simply that the wind speed and/or direction changed during the time between the radiosonde sounding (1010 EST) and Doppler data (roughly 1120 and 1220). This seems rather unlikely in light of the short time involved between the two measurements. A third possibility involves a change in the wind field with distance. Note that the Doppler data were taken at distances from 31.0 to 125.3 km from the radiosonde launcher.

In Runs 2 and 3 we have a different situation. Two of the gates in Run 2 have variations in the mean Doppler which are greater than those expected for the pulse volume altitude interval. In Run 3, none of the measured frequencies correspond to the expected values. The only satisfactory explanation in these cases would appear to be a change in the wind field with either time or distance.

c. *Reflectivity factor*

The reflectivity factor for each of the 10-sec intervals was calculated using the area under the Doppler spectra as the received signal intensity and assuming the particles were ice crystals at all altitudes. No amplitude data were recorded at either X or S band. A correction was made to account for noise. The reflectivity factor varied as much as an order of magnitude during the 1–2 min runs. The average value for each run is shown in Table 1. As noted above, there is some evidence that the pulse volumes may not be filled so that the reflectivity factors shown are minimum values. Unfortunately, the highest altitude where Doppler data were taken was around 6 km so that no estimates of reflectivity at the generating level itself is possible. It is of interest, nevertheless, to compare the present reflectivity factor measurements with those of previous investigators in similar natural cloud forms.

Plank *et al.* (1955) made reflectivity measurements in a variety of cloud types. In mares tail cirrus, which was barely detectable with their 1.25 cm radar, they estimate a reflectivity factor around 3 $mm^6\ m^{-3}$. In cirrus filosus, similar to cirrus uncinus, their values vary from 20 to 50 $mm^6\ m^{-3}$ through the cloud deck which extended from 20,000 to 25,000 ft. Heymsfield and Knollenberg (1972) measured particle size spectra during repeated passes through cirrus uncinus generating cells in both Colorado and Minnesota. Based on these spectra, the reflectivity factor was calculated. In Minnesota the maximum value measured was 17.1 $mm^6\ m^{-3}$. Somewhat higher values were found in the Colorado flights—36.0 maximum and 17.0 average.

Now the effect of wind shear and sorting due to fall velocity as outlined by Douglas *et al.* (1957) and Gunn and Marshall (1955) is to diffuse the trail and reduce the reflectivity factor with distance below the generating element. If we assume that some diffusion of the filament took place, then the reflectivity factor at the generating level at 9 km is higher than that measured at 6.2 km. Further, if we consider the possibility of the beam not being filled during Run 1 at 6.2 km, then the estimated reflectivity factor in the generator could be considerably higher than those measured previously by radar and aircraft.

d. *Terminal fallspeeds*

An attempt was made to calculate the fallspeed of the particles using the elemental approach discussed by Marshall (1953). Several difficulties arise in attempting such an approach. First is the obvious difficulty in measuring pattern slope on the RHI photographs. In most cases, the radar returns were very strong and bloomed the scope. Further, slope measurements must be made over an altitude increment rather than at a point. The most serious difficulties, however, are due to the three-dimensionality of the streamers. In the simple development by Marshall (1953), the wind is considered to be from only one direction at all heights and the wind speed to increase linearly with height, i.e., constant wind shear. The particle trail is contained in a single vertical plane and slope measurements provide a true measure of fallspeed. In the present case, however, the trail is three dimensional due to the variation in both wind speed (shear) and direction with height. Further, the generating line, i.e., the condensation trail, was not laid perpendicular to the wind at that altitude. The actual aircraft tracks are not known but the jet route generally parallels the coast along a 20°–200° line. The winds at the generating level, around 9 km, were from 240°–250°. Douglas *et al.* (1957) discuss the three-dimensional problem and the effect on fallspeed calculations based on slope measurements from time-height radar records.

The final problem concerns the height of the generating line, i.e., the flight altitudes of the jet aircraft. Where the wind field is unidirectional with constant shear, the height of the generating element does not affect the *shape* of the trail in the sense that all trails are parabolic. Where the wind field varies in both direction and shear with altitude, the shape of the

trail is highly dependent on the height of the generating line.

In light of the above limitations to the data it was decided not to attempt a full three-dimensional solution for the fallspeed such as described by Miles (1956) or Douglas *et al.* (1957). Instead the wind field was divided into sections where the variation in wind speed and direction with height approximated that for the simpler two-dimensional solution.

Fallspeed calculations were made in two regions: 1) that between the generating level, around 9 km, and the upper slope reversal in the S-shaped pattern at 8 km and 2) that between the lower slope reversal at around 7 to 4 km. In these two regions the wind direction and slope of the wind speed are roughly constant. It should be noted that the two points where the pattern slope becomes vertical may be considered as "apparent generating levels." Thus, for the lower region, the generating level was taken at 7 km.

The PPI photographs show that the streamers are oriented generally along an E–W direction (see Figs. 10 and 11). This was taken to be the plane of the trail. Measured slopes taken from RHI's at azimuths other than 90° were corrected to account for the cross-plane effect discussed above.

The results of the fallspeed calculations for the two altitude regions are shown in Fig. 14. The points range from 0.4 to 1.4 sec^{-1} with no apparent variation with altitude. This small spread in the fallspeeds is somewhat surprising considering the limitations to the data and approximations made. A number of investigators have measured fallspeeds based on the pattern slopes. Marshall (1953) and Langleben (1956) found fallspeeds around 1 m sec^{-1} based on trail slopes using time-height records. Atlas (1957) examined the structure of an isolated streamer and measured fallspeeds ranging from 1.7 to 2 m sec^{-1}. The spread in fallspeeds reported by Douglas *et al.* (1957) was quite large, from 0.3 to 3 m sec^{-1}. This large spread, however, was attributed to the effects of the orientation of the generating line and wind shear relative to the direction of motion of the generating element.

A direct measure of fallspeed spreads in precipitation streaks was made by Probert-Jones (1960) with a vertically pointing Doppler radar. The outstanding feature of these measurements was the high fall velocity, 3 to 4 m sec^{-1}, and the very narrow width of the velocity spectra. He suggests that the particles were graupel or small hail.

The properties of ice crystals have been measured in both cirrus clouds (Heymsfield and Knollenberg, 1972), and condensation trails (Knollenberg, 1972). The measurements in natural cirrus show that the crystals are almost exclusively bullets and rosettes in the generating cells. Mean crystal lengths measured in the "heads" of cirrus uncinus varied from 0.5 to 1 mm with maximum values of 2 mm. In the contrail,

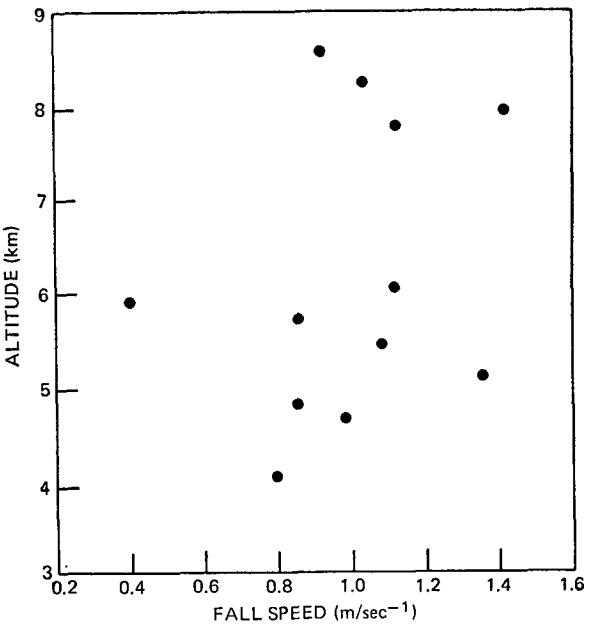

FIG. 14. Fallspeeds as determined from pattern slopes.

however, the crystals were somewhat smaller with mean values around 0.2 to 0.4 mm and a maximum of 1.3 mm.

Terminal velocities for various crystal types have been calculated most recently by Heymsfield (1972) and compared to available experimental data. Assuming the ice crystals in the contrail to be bullets, the fallspeeds calculated from the pattern slopes correspond to bullet lengths of 0.6 to 1.0 mm. Thus, the contrail streamers appear to have crystal sizes approximating natural cirrus uncinus. This may well be a reasonable conclusion. Knollenberg's measurements were made in the contrail itself shortly after it was laid. In the present case, the radar data were taken in streamers well below the generating level. Further, the generating line (the contrail) was originally laid several hours prior to the radar observations as discussed above. Thus, it appears that while the condensation trail provided the trigger for the development of a generating line and the streamers, the generating mechanism continued to develop, following this initial trigger, as in naturally occurring cirrus cloud formation. A question arises, however, concerning the reliability of the fall velocity calculations for bullets by Heymsfield. He notes that the only measured terminal velocities for bullets were by Bashkirova and Pershina (1964) at an unspecified altitude so that very little experimental data are available to confirm his theoretical calculations.

An alternate explanation may be simply that the larger crystals fall out while the small crystals are left to grow in the generating line. Such a process is suggested by Knollenberg to explain the size distributions found in the contrail.

4. Conclusions

The observations graphically illustrate the potential effect of condensation trails on the lower atmosphere. The streamers emanating from the contrails provide a rich source of ice crystals which may act as natural seeding elements. Conversely, as occurred on this day, the crystals may simply fall through the entire region below the generating level without triggering any additional precipitation. Certainly, the fact that the generating elements or lines continued to be active for several hours—producing streamers which reached from the generating level to the ground—is most striking. In this regard, high-power radar and perhaps lidar are the only remote probes which are capable of detecting the weak returns from these streamers, particularly in the lower reaches of the atmosphere where the streamers are somewhat diffuse with low reflectivities. The implications of these observations are open to conjecture but certainly further research into artificially generated cirrus via condensation trails and its effect on the lower atmosphere is indicated.

Acknowledgments. This research has been supported by the Air Force Cambridge Research Laboratories and by the National Aeronautics and Space Administration, Wallops Island. The authors are grateful to the personnel of the JAFNA radar facility for their cooperation during the various observations and experiments.

REFERENCES

Appleman, H., 1953: The formation of exhaust condensation trails by jet aircraft. *Bull. Amer. Meteor. Soc.*, **31**, 14–20.

Atlas, D., 1957: Drop size and radar structure of a precipitation streamer. *J. Meteor.*, **14**, 261–271.

Bashkirova, G., and T. Pershina, 1964: On the mass of snow crystals and their fall velocities. *Tr. Gl. Geofiz. Observ.*, No. 165, 83–100.

Braham, R. R., and P. Spyers-Duran, 1967: Survival of cirrus crystals in clear air. *J. Appl. Meteor.*, **6**, 1053–1061.

Browne, I. C., 1952: Precipitation streaks as a cause of radar upper bands. *Quart. J. Roy. Meteor., Soc.*, **78**, 590–595.

Douglas, R. H., K. L. S. Gunn and J. S. Marshall, 1957: Pattern in the vertical of snow generation. *J. Meteor.*, **14**, 95–114.

Gunn, K. L. S., and J. S. Marshall, 1955: The effect of wind shear on falling precipitation. *J. Meteor.*, **12**, 339–349.

Gunn, R., M. P. Langleben, A. S. Dennis and B. A. Pewer, 1954: Radar evidence of a generating level for snow. *J. Meteor.*, **11**, 20–23.

Heymsfield, A. J., 1972: Ice crystal terminal velocities. *J. Atmos. Sci.*, **29**, 1348–1357.

——, and R. G. Knollenberg, 1972: Properties of cirrus generating cells. *J. Atmos. Sci.*, **29**, 1358–1366.

Knollenberg, R. G., 1972: Measurements of the growth of the ice budget in a persisting contrail. *J. Atmos. Sci.*, **29**, 1367–1374.

Langleben, M. P., 1956: The plan pattern of snow echoes at the generating level. *J. Meteor.*, **13**, 554–560.

Lhermitte, R., 1952: Les "bandes superieures" dans la structure vertical des echoes de pluie. *C. R. Acad. Sci.*, **235**, 1414–1416.

Marshall, J. S., 1953: Precipitation trajectories and patterns. *J. Meteor.*, **10**, 25–29.

——, W. Hitschfeld and K. L. S. Gunn, 1955: *Advances in Geophysics.* Vol. 2, New York, Academic Press, 1–56.

Mason, B. J., 1971: *The Physics of Clouds.* Oxford, Clarendon Press, 468–470.

Miles, V. G., 1956: Interpretation of the height-versus-time presentation of radar echoes. *J. Meteor.*, **13**, 362–368.

NCAR, 1969: *Facilities for Atmospheric Research.* No. 11, 16–17.

Plank, V. G., D. Atlas and W. H. Paulsen, 1955: The nature and detectability of clouds and precipitation as determined by 1.25-centimeter radar. *J. Meteor.*, **12**, 358–378.

Probert–Jones, J. R., 1960: The analysis of Doppler radar echoes from precipitation. *Preprints 8th Weather Radar Conf.*, Miami, Fla., Amer. Meteor. Soc., 347–354.